Contribution from the Department of Chemistry, University of Houston—University Park, Houston, Texas 77004, and Laboratoire de Synthèse et d'Electrosynthèse Organométallique associé au CNRS (UA 33), Faculté des Sciences "Gabriel", University of Dijon, 21100 Dijon, France

Electrochemical Studies of Monomeric Niobium(V) and Niobium(IV) Porphyrins in Nonaqueous Media

J. E. Anderson,[1a] Y. H. Liu,[1a] R. Guilard,[1b] J. M. Barbe,[1b] and K. M. Kadish*[1a]

Received May 13, 1986

The redox properties of five monomeric Nb(V) and Nb(IV) metalloporphyrins were investigated in nonaqueous media. The compounds studied were (P)Nb^{V}(O)(L) and (P)Nb^{IV}(O) where P is the dianion of tetraphenylporphyrin (TPP), the dianion of octaethylporphyrin (OEP), or the dianion of tetra-*p*-tolylporphyrin (TpTP) and L is acetate anion ($O_2CCH_3^-$) or acetylacetonate anion ($acac^-$). The investigated niobium(V) porphyrins could be reduced by up to three electrons and oxidized by one electron. Chemical reactions followed both the reduction and the oxidation of the niobium(V) complexes. The niobium(IV) porphyrins could be reduced by up to two electrons and oxidized by two electrons. Reductions of the niobium(IV) complexes were reversible, but chemical reactions followed the oxidations. Each electrode reaction was monitored by spectroelectrochemistry and ESR spectroscopy, and on the basis of these data an overall mechanism for the oxidation and reduction of monomeric Nb(V) and Nb(IV) porphyrins is presented.

Introduction

Numerous monomeric niobium(IV) and niobium(V) porphyrin complexes have been reported. Monomeric niobium(IV) porphyrins include (P)Nb(O),[2] (P)$Nb(X)_2$,[3] (P)Nb(O)(O_2),[4,5] and (P)$Nb(X)_2(O_2)$.[6] The last two complexes are the dioxygen adducts of the first two complexes. Although formally a Nb(IV) species, (P)$Nb(X)_2(O_2)$ has been described[6] as containing Nb(V)–$O_2^{\bullet}$ on the basis of ESR data. Monomeric niobium(V) porphyrins are characterized by (P)Nb(O)(X) and (P)$Nb(X)_3$, where X is a halogen.[6-10] The X-ray crystal structures of (P)Nb(O)(F)[10] and (P)Nb(O)(O_2CCH_3)[11,12] indicate that the nonporphyrin ligands assume a cis geometry around the niobium atom, which is above the plane of the porphyrin macrocycle.

Very little electrochemistry has been published on niobium porphyrins, and no complex has ever been characterized with respect to both oxidation and reduction under the same experimental conditions. The reductive electrochemistry of (P)Nb(O)(O_2CCH_3),[2,3,13] (P)Nb(O)(F),[2] and (P)Nb(O)[2] has been reported, but a complete spectroscopic characterization of the reaction products has not been published. In addition, contrasting interpretations of the electrochemical data have been presented for the acetate monomer. In one paper, the first two reductions are reported to occur at the Nb center,[13] while another paper[2] reports that only the first reduction is metal-centered while the second occurs at the porphyrin π ring system. The discrepancies between these two proposed mechanisms will be addressed in this present paper.

Here, we also report the electrochemistry of (TPP)Nb(O), (TpTP)Nb(O)(O_2CCH_3), (OEP)Nb(O)(O_2CCH_3), and (TPP)Nb(O)(L), where L is an acetate anion ($O_2CCH_3^-$) or an acetylacetonate anion ($acac^-$). The combination of data from various electrochemical techniques with data from spectroelectrochemistry and ESR spectroscopy enables the formulation of an overall oxidative and reductive mechanism for these species. In addition, the electrochemical properties of the Nb(V) monomers are compared with those of the Nb(V) dimers.[14]

Experimental Section

Materials. Reagent grade benzonitrile (PhCN) was vacuum-distilled from P_2O_5. Butyronitrile (*n*-PrCN) was predried with $CaCl_2$. Spectroscopic grade pyridine (py) was twice distilled from CaH_2. HPLC grade dichloromethane (CH_2Cl_2) was distilled from P_2O_5. Reagent grade tetrahydrofuran (THF) was distilled first from CaH_2 and then from Na and benzophenone. All solvents were distilled either under an inert atmosphere (py, THF, CH_2Cl_2, *n*-PrCN) or vacuum-distilled (PhCN) just prior to use. Tetra-*n*-butylammonium perchlorate (TBAP) was purchased from Eastman Kodak Co., purified by two recrystallizations from ethyl alcohol, and stored in a vacuum oven at 40 °C. Unless otherwise noted, 0.2 M tetrabutylammonium perchlorate (TBAP) was used as supporting electrolyte for cyclic voltammetric measurements, bulk solution electrolysis, and spectroelectrochemical measurements. The monomeric niobium porphyrin species studied were synthesized and purified by methods already reported.[3,6-11]

Instrumentation and Methods. All electrochemical measurements, with the exception of spectroelectrochemistry, were performed by Schlenk techniques. Cyclic voltammetric and polarographic measurements were obtained with either an IBM EC225 voltammetric analyzer or an EG&G Princeton Applied Research Model 174A/175 polarographic analyzer/potentiostat. This latter instrument was coupled with an EG&G Model 9002A X-Y recorder for potential scan rates less than 500 mV/s or a Tektronix 5111 storage oscilloscope for scan rates equal to or larger than 500 mV/s. UV–visible spectra were recorded on an IBM 9430 spectrophotometer or a Tracor Northern 1710 holographic optical spectrometer/multichannel analyzer. ESR measurements were performed with ESR cells modified for use with a Schlenk line. ESR spectra were recorded on an IBM Model ED-100 electron spin resonance system.

Platinum working and counter electrodes were used for all electrochemical measurements. In the case of the thin-layer spectroelectrochemical cell, a platinum minigrid electrode was used. A saturated calomel electrode (SCE) that was separated from the bulk of the solution by a fritted-glass disk junction was used as the reference electrode. The ferrocene/ferrocenium (Fc/Fc^+) couple was also used as an internal standard for potential measurements. Low-temperature experiments were performed by use of a dry ice/acetone bath to cool the cell to a constant temperature, monitored with a thermocouple. Bulk controlled-potential coulometry was carried out with an EG&G Princeton Applied Research Model 173 potentiostat/179 coulometer system, coupled with an EG&G Model RE 0074 time-based X-Y recorder. Thin-layer spectroelectrochemical measurements were made with an IBM EC225 voltammetric analyzer coupled with a Tracor Northern 1710 spectrometer/multichannel analyzer.

(1) (a) University of Houston. (b) University of Dijon.
(2) Guilard, R.; Richard, P.; El Borai, M.; Laviron, E. *J. Chem. Soc., Chem. Commun.* **1980**, 516.
(3) Richard, P.; Guilard, R. *Nouv. J. Chim.* **1985**, *9*, 119.
(4) Matsuda, Y.; Sakamoto, S.; Takaki, T.; Murakami, Y. *Chem. Lett.* **1985**, 107.
(5) Matsuda, Y.; Sakamoto, S.; Koshima, H.; Murakami, Y. *J. Am. Chem. Soc.* **1985**, *107*, 6415.
(6) Richard, P.; Guilard, R. *J. Chem. Soc., Chem. Commun.* **1983**, 1454.
(7) Buchler, J. W.; Rohbock, K. *Inorg. Nucl. Chem. Lett.* **1972**, *8*, 1073.
(8) Gouterman, M.; Hanson, L. K.; Khalil, G.-E.; Buchler, J. W.; Rohbock, K.; Dolphin, D. *J. Am. Chem. Soc.* **1975**, *97*, 3142.
(9) Green, M. L. H.; Moreau, J. J. E. *Inorg. Chim. Acta* **1978**, *31*, L461.
(10) Lecomte, C.; Protas, J.; Richard, P.; Barbe, J. M.; Guilard, R. *J. Chem. Soc., Dalton Trans.* **1982**, 247.
(11) Lecomte, C.; Protas, J.; Guilard, R.; Fliniaux, B.; Fournari, P. *J. Chem. Soc., Dalton Trans.* **1979**, 1306.
(12) Lecomte, C.; Protas, J.; Guilard, R.; Fliniaux, B.; Fournari, P. *J. Chem. Soc., Chem. Commun.* **1976**, 434.
(13) Matsuda, Y.; Yamada, S.; Goto, T.; Murakami, Y. *Bull. Chem. Soc. Jpn.* **1981**, *54*, 452.
(14) Anderson, J. E.; Liu, Y. H.; Guilard, R.; Barbe, J. M.; Kadish, K. M. *Inorg. Chem.* **1986**, *25*, 2250.

0020-1669/86/1325-3786$01.50/0

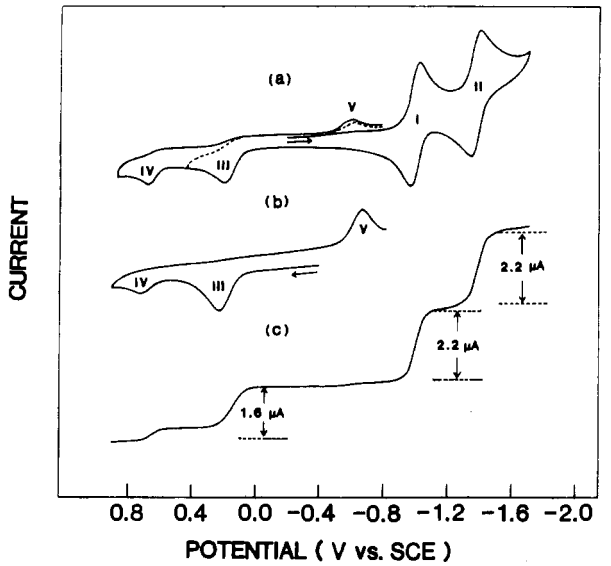

Figure 1. (a) Cyclic voltammograms of (TPP)Nb(O) in 0.2 M TBAP, CH_2Cl_2. Scan rate = 0.1 V/s. (b) Thin-layer cyclic voltammogram of (TPP)Nb(O) in 0.2 M TBAP, CH_2Cl_2. Scan rate = 0.01 V/s. (c) Rotating-disk voltammogram of (TPP)Nb(O) in 0.2 M TBAP, CH_2Cl_2. Rotation rate = 300 rpm.

Table I. Potentials (V vs. SCE) for Reduction and Oxidation of (TPP)Nb(O) in CH_2Cl_2, Pyridine, and PhCN Containing 0.2 M TBAP[a]

	Nb(V)/Nb(IV)			porphyrin ring reduction	
solvent	peak III[b]	peak IV[b]	peak V[c]	peak I	peak II
CH_2Cl_2	0.18	0.66	−0.62	−1.01	−1.39
pyridine	0.06		−0.80	−0.95	−1.38
PhCN	0.20	0.60	−0.60	−0.98	−1.43

[a] See Figure 1. [b] Irreversible oxidation. E_p given at a scan rate of 0.10 V/s. [c] Irreversible reduction, which was observed only after scanning the potential positive of peak III or peak IV. E_p given at a scan rate of 0.10 V/s.

Results and Discussion

Electrochemistry of (TPP)Nb(O). A cyclic voltammogram of (TPP)Nb(O) in CH_2Cl_2, 0.2 M TBAP is shown in Figure 1a. Two reversible one-electron reductions (processes I and II, Figure 1a) occur at $E_{1/2} = -1.01$ V and $E_{1/2} = -1.39$ V. Both processes I and II are characterized by an $|E_{pa} - E_{pc}| = 60 \pm 5$ mV. The ratio of $i_p/v^{1/2}$ is constant for both waves, indicating diffusion-controlled processes. This is similar to what has been previously reported.[2]

Figure 1a shows the presence of two oxidation peaks and one coupled rereduction peak upon scanning the potential in a positive direction. The potentials for these reactions depend upon scan rate, and at a scan of 0.1 V/s the two irreversible oxidations of (TPP)Nb(O) are observed at $E_p = 0.18$ V and $E_p = 0.66$ V. These peaks are labeled III and IV in Figure 1a. These oxidations are coupled to an irreversible reduction peak that, at 0.1 V/s, occurs at $E_p = -0.62$ V. This peak is labeled peak V in Figure 1a. The same three peaks are also observed by thin-layer electrochemistry (Figure 1b). The three irreversible peaks in Figure 1a,b have not previously been reported for (TPP)Nb(O) or for any other Nb(IV) or Nb(V) porphyrin. However, an irreversible oxidation peak has been reported for (OEP)Nb(O) at $E_p = 0.55$ V in THF.[2] Reduction peak V is not observed unless the potential is first scanned past oxidation peak III. Also, currents for peak V are slightly higher when the potential is scanned past the second oxidation peak (peak IV) at $E_p = 0.66$ V. Thus, this reduction process is clearly associated with the two oxidations.

The second of the two oxidation processes (peak IV, Figure 1a) has smaller currents than the first process and is not observed in pyridine nor is it observed when (P)Nb(O) is electrochemically generated from (P)Nb(O)(O_2CCH_3) in situ. The exact nature of the two reactive species leading to processes III and IV is not known. The potential for peak III is solvent-dependent (see Table I), shifting from $E_p = 0.18$ V in CH_2Cl_2 to $E_p = 0.06$ V in pyridine at a scan rate of 0.1 V/s. This supports the assignment of solvated Nb(IV) as one of the reacting species in binding solvents and suggests that the two oxidations may be due to a solvated and an unsolvated species. This also implies that both oxidations in Figure 1 are due to a metal-centered Nb(IV)/Nb(V) reaction. The negative potentials of these oxidations, the irreversible nature of the oxidations, and the known chemical oxidation of (P)Nb(O) to generate a Nb(V) species[3] all support this assignment. In addition, bulk electrolysis at either 0.4 or 0.8 V gives the same Nb(V) species, which is characterized by UV–visible bands at 410 and 445 nm. However, it should be noted that the sum of the oxidation current for processes III and IV is less than that for either process I or II.

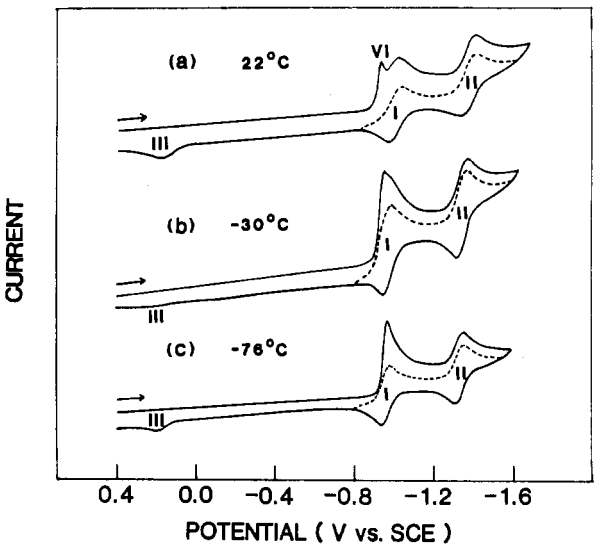

Figure 2. Cyclic voltammograms of 1×10^{-3} M (TPP)Nb(O)(O_2CCH_3) solution in CH_2Cl_2, 0.2 M TBAP at (a) 22 °C, (b) −30 °C, and (c) −76 °C. Scan rate = 0.1 V/s.

The two reversible reductions (waves I and II) have equal currents (see Figure 1c) and have been described as consecutive one-electron additions to the porphyrin ligand.[2] Reduction peak V is only observed after oxidation of (P)Nb(O) and is assigned as due to a Nb(V)/Nb(IV) reduction. The irreversible nature of this process suggests a chemical reaction following reduction. However, the potentials of processes I and II are not shifted on the second scan, suggesting that (TPP)Nb(O) is formed as a final product of this chemical reaction.

Reduction of (P)Nb(O)(O_2CCH_3). Figure 2 illustrates cyclic voltammograms of (TPP)Nb(O)(O_2CCH_3) at three different temperatures in CH_2Cl_2, 0.2 M TBAP. At room temperature, the voltammogram is similar to but not identical with that reported in the literature.[2,3] This voltammogram is shown in Figure 2a. An irreversible reduction is observed at $E_p = -0.94$ V (peak VI), and this process overlaps with another reversible reduction at $E_{1/2} = -1.00$ V (peak I).

The irreversible nature of the first reduction (peak VI) is best illustrated by voltammograms taken on the first and the second potential sweeps between −0.6 and −1.6 V. The reduction at $E_p = -0.94$ V is not observed on the second sweep (dotted line, Figure 2), but the reaction at $E_{1/2} = -1.0$ V remains well defined and has currents equal to those of the third reduction at $E_{1/2} = -1.38$ V. The overall reductive behaviors of (P)Nb(O)(O_2CCH_3), where P = TPP, OEP, and TpTP, are similar, and Table II lists the reduction and oxidation potentials for these compounds in different solvents and at different temperatures.

Formation of (TPP)Nb(O) upon the one-electron reduction of (TPP)Nb(O)(O_2CCH_3) is best demonstrated by the electrochemistry. The second and third reductions of (TPP)Nb(O)(O_2CCH_3) (peaks I and II) are at the same potentials as peaks I and II of (TPP)Nb(O). Also, both the Nb(V) and the Nb(IV)

Table II. Potentials (V vs. SCE) for Reduction and Oxidation of (P)Nb(O)(O_2CCH_3) and (TPP)Nb(O)(acac) in Various Solvents Containing 0.2 M TBAP[a]

compd	solvent	temp, °C	Nb(V)/Nb(IV) peak VI[b]	Nb(V)/Nb(IV) peak III[b]	ring redn peak I	ring redn peak II	ring oxidn peak VIII
(OEP)Nb(O)(O_2CCH_3)	THF	22	−1.07	−0.01	−1.15	−1.52	1.06[b]
		−75	−1.20	0.00	−1.17	−1.53	1.07
	CH_2Cl_2	22	−1.18	0.05	−1.24	−1.71	0.98
		−75	−1.23	0.11	−1.20	−1.67	0.98
	PhCN	22	−1.16	0.05	−1.25	−1.71	0.98
	n-PrCN	22	−1.16	−0.02	−1.24	−1.70	1.01
		−75	−1.24	0.00	−1.21	−1.66	1.00
	pyridine[c]	22	−1.10	−0.11	−1.20	−1.62	
(TpTP)Nb(O)(O_2CCH_3)	THF[c]	22	−0.92	0.14	−0.97	−1.37	
	CH_2Cl_2[c]	22	−0.98	0.20	−1.02	−1.41	1.15
	PhCN[c]	22	−0.95	0.17	−1.01	−1.46	1.19
(TPP)Nb(O)(O_2CCH_3)	THF[c]	22	−0.88	0.10	−0.93	−1.33	
	CH_2Cl_2	22	−0.94	0.17	−1.00	−1.38	1.21
		−76	−0.96	0.20	−0.95	−1.33	1.21
	PhCN[c]	22	−0.90	0.16	−0.97	−1.41	1.23
	pyridine[c]	22	−0.89	0.02	−0.95	−1.36	
	Me_2SO[c]	22	−0.80	−0.10	−0.87	−1.27	
(TPP)Nb(O)(acac)	THF	22	−1.09	0.14	−0.91	−1.33	
		−60	−1.12		−0.94	−1.32	1.17
	CH_2Cl_2	22	−1.18	0.18	−1.00	−1.39	1.03
		−74	−1.14	0.27	−0.95	−1.32	1.05

[a] See Figure 2. [b] E_p at a scan rate of 0.1 V/s. [c] 0.1 M TBAP.

complexes show an irreversible oxidation peak III. As seen in Table II, the exact potential of this peak is solvent-dependent and this behavior is identical with that for peak III of (TPP)Nb(O).

Figure 2b,c shows the changes that occur in the reduction of (TPP)Nb(O)(O_2CCH_3) upon decreasing the temperature from +22 to −76 °C. At −30 °C the first reduction peak has shifted negatively such that it almost completely overlaps the second reversible reduction at $E_{1/2} = -1.00$ V. This negative shift continues as the temperature is lowered, and at −76 °C a complete overlapping of the two processes has occurred. This is shown in Figure 2c. The current for the first reduction is approximately double that of the second reduction, but both peaks are equal in height after reversing the sweep and scanning a second time in a negative direction. This is indicated by the dotted line in Figure 2c.

The addition of one electron to different monomeric Nb(V) porphyrins has been characterized by both ESR and UV–visible data and has been described as a reduction at the metal to form a Nb(IV) species.[2,13] In this present study, controlled-potential reduction of (TPP)Nb(O)(O_2CCH_3) was performed stepwise at −0.94 V, −1.08 V, and −1.52 V, and the spectra obtained after each one-electron reduction are shown in Figure 3. The first reduction generates a spectrum characteristic of (P)Nb(O). The Soret band at 430 nm slightly decreases in intensity, while the band at 533 nm shows a larger decrease in intensity. The band at 555 nm increases in intensity, and a new band at 596 nm is formed. This is shown in Figure 3a, and the UV–visible spectral data for singly reduced (TPP)Nb(O)(O_2CCH_3) and (OEP)Nb(O)(O_2CCH_3) are presented in Table III. The same basic changes in spectra are observed for all three of the (P)Nb(O)(O_2CCH_3) complexes studied.

Spectroelectrochemical monitoring of the reduction products shows that the addition of a second electron to (P)Nb(O)(O_2CCH_3) corresponds to formation of a porphyrin π anion radical. When (TPP)Nb(O)(O_2CCH_3) is reduced at a controlled potential of −1.08 V, the Soret band drops in intensity, broadens, and shifts to 440 nm. The bands at 555 and 596 nm also drop in intensity during electroreduction, and a new band appears at 718 nm. The initial changes in the UV–visible spectrum indicate that (P)Nb(O) is formed in the first step and that the overall addition of two electrons yields [(P)Nb(O)]$^-$ as a final product.

The third reduction of (P)Nb(O)(O_2CCH_3) is a reversible, one-electron transfer on the cyclic voltammetric time scale. Upon controlled-potential reduction of (TPP)Nb(O)(O_2CCH_3) at −1.52 V, the Soret band at 440 nm further reduces in intensity. The band at 718 nm disappears, and new bands are formed at 559 and 605 nm. These changes in the UV–visible spectra during controlled-potential reduction indicate[15] that the addition of a third

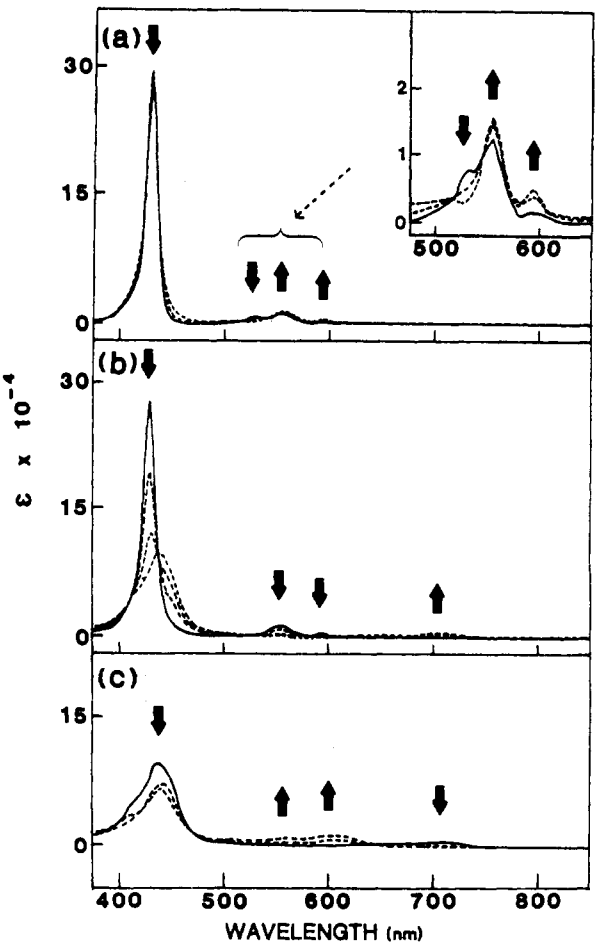

Figure 3. Thin-layer electronic absorption spectra of (TPP)Nb(O)(O_2CCH_3) in PhCN, 0.2 M TBAP (a) during controlled-potential reduction at −0.94 V, (b) after stepping the potential from −0.94 to −1.08 V, and (c) after stepping the potential from −1.08 to −1.52 V.

(15) For examples see: Kadish, K. M. *Prog. Inorg. Chem.* **1986**, *34*, 435–605.

Table III. Absorption Maxima (nm) and Molar Absorptivities (ϵ) of Neutral and Reduced (OEP)Nb(O)(O_2CCH_3) and (TPP)Nb(O)(O_2CCH_3) in THF and PhCN, Respectively, Containing 0.2 M TBAP

	λ_{max}, nm ($10^{-4}\epsilon$)			
compd	neutral	red 1[a]	red 2[b]	red 3[c]
(OEP)Nb(O)(O_2CCH_3)	410 (12.7)	407 (22)	408 (8.8)	414 (4.5)
	522 (0.6)	538 (1.3)	414 (8.8)	455 (3.0)
	538 (1.0)	575 (1.8)	631 (1.8)	538 (1.1)
	565 (1.5)		665 (0.9)	582 (1.6)
	583 (1.0)		806 (0.7)	769 (0.6)
(TPP)Nb(O)(O_2CCH_3)	430 (29.7)	430 (27.8)	440 (9.9)	442 (6.9)
	533 (0.8)	555 (1.6)	718 (0.7)	559 (1.2)
	555 (1.2)	596 (0.5)		605 (1.5)

[a] Spectra obtained after controlled-potential reduction at rising portion of peak VI. [b] Spectra obtained after controlled-potential reduction at potentials between peak I and peak II. [c] Spectra obtained after controlled-potential reduction at potentials negative of peak II.

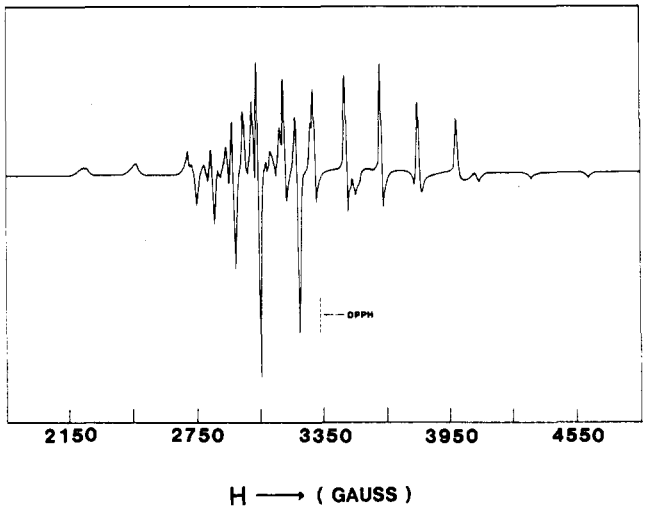

Figure 4. ESR spectrum obtained during reduction of (OEP)Nb(O)(O_2CCH_3) at an applied potential of −1.2 V in THF, 0.2 M TBAP.

electron is at the porphyrin π ring system, forming the Nb(IV) dianion, $[(TPP)Nb(O)]^{2-}$.

The second and third reductions of (TPP)Nb(O)(O_2CCH_3) are spectrally reversible, and the stepwise reoxidation of $[(TPP)Nb(O)]^{2-}$ first at −1.27 V and then at −0.8 V generates the (TPP)Nb(O) species. The UV–visible spectrum of (TPP)Nb(O)(O_2CCH_3) is not observed by controlled-potential reoxidation at −0.80 V, but upon reoxidation at 0.20 V the original starting material is regenerated. This is consistent with oxidation peak III being the Nb(IV)/Nb(V) reaction.

ESR spectra obtained from frozen solutions of (P)Nb(O)(O_2CCH_3) that had been electrolysized at potentials between peak I and II are very sensitive to the total time of reduction. Also, an accurate measurement of the number of electrons added is difficult, due to an overlap of the first two reduction waves and the irreversibility of process VI. The first ESR signal observed is from (P)Nb(O) and is shown in Figure 4 for reduction of (OEP)Nb(O)(O_2CCH_3). An ESR signal is observed up to the addition of about 1.0 electron per monomer, but the intensity of this signal decreases as a function of continued electrolysis time. This may indicate the formation of an ESR-silent species. However, when approximately two electrons have been added to the monomer, a strong free-radical species is observed in the ESR spectrum. The signal has a g value of 2.003 and a signal width of 8 G. The signal is similar to that assigned to $[(TPP)Nb(O)]^{3-}$ by Matsuda et al.[13] Upon longer periods of electrolysis, this free-radical signal decreases in intensity. The nature of the species that gives the free-radical signal is unknown. Finally, when an ESR measurement is performed on a frozen solution of (OEP)Nb(O)(O_2CCH_3) that has been electrolysized at −1.7 V in THF, the predominant, stable ESR signal obtained is identical with that reported[3] for (OEP)Nb(O) and most likely corresponds to the signal of $[(OEP)Nb(O)]^{2-}$.

The second reduction of (P)Nb(O)(O_2CCH_3) has been reported to be both a ring[2] and metal-centered[13] reduction. The latter

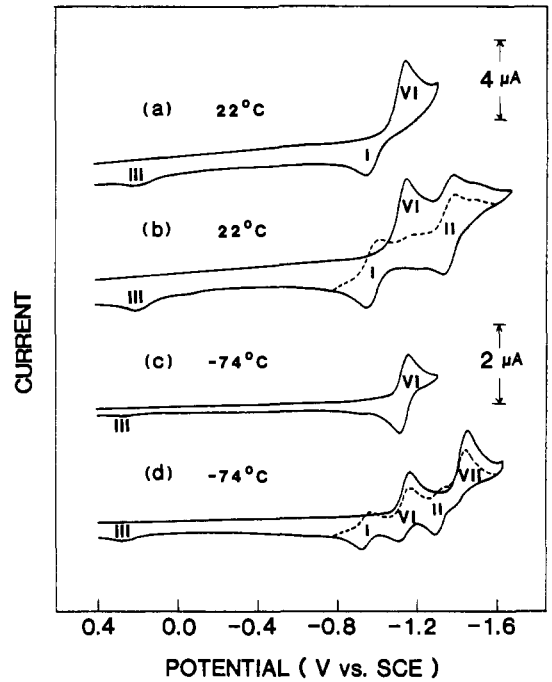

Figure 5. Cyclic voltammograms of 1×10^{-3} M (TPP)Nb(O)(acac) in 0.2 M TBAP: (a) single scan at 22 °C; (b) first and second scans at 22 °C; (c) first scan at −74 °C; (d) first and second scans at −74 °C. Scan rate = 0.1 V/s.

assignment was based, in part, on ESR data that showed a free-radical signal after reduction of (TPP)Nb(O)(O_2CCH_3) at −1.46 V vs. SCE. This potential is at the peak potential of the third reduction of (TPP)Nb(O)(O_2CCH_3), and the signal was thus assigned as due to $[(TPP)Nb(O)]^{3-}$. Because the addition of three electrons to (TPP)Nb(O)(O_2CCH_3) gave a species with a free-radical signal rather than a Nb(IV) signal, it was reasoned that the first two reductions must be at the metal center, i.e. Nb(V)/Nb(IV) and Nb(IV)/Nb(III). However, as already indicated, a fast chemical reaction follows the initial reduction. ESR experiments that give information about the reaction products should therefore be coupled with other spectroscopic techniques. This did not appear to be the case in the reported ESR spectral studies that gave the assignment of Nb(III).[13]

Reduction of (TPP)Nb(O)(acac). Room-temperature cyclic voltammograms of (TPP)Nb(O)(acac) in CH_2Cl_2, 0.2 M TBAP are shown in Figure 5a,b and potentials are summarized in Table II. Two reduction processes are observed. The first (peak VI) is irreversible and occurs at $E_p = -1.18$ V. A reoxidation process at $E_p = -0.97$ V is coupled to this first irreversible wave. This peak is assigned as peak I. The second reduction (peak II) is reversible and occurs at $E_{1/2} = -1.39$ V. The reversible wave is characterized by an $|E_{pa} - E_{pc}| = 60 \pm 5$ mV and a constant value of $i_p/v^{1/2}$, thus suggesting a one-electron diffusion-controlled process. The current for the first reduction is twice that of the second reduction from rotating-disk experiments and suggests a

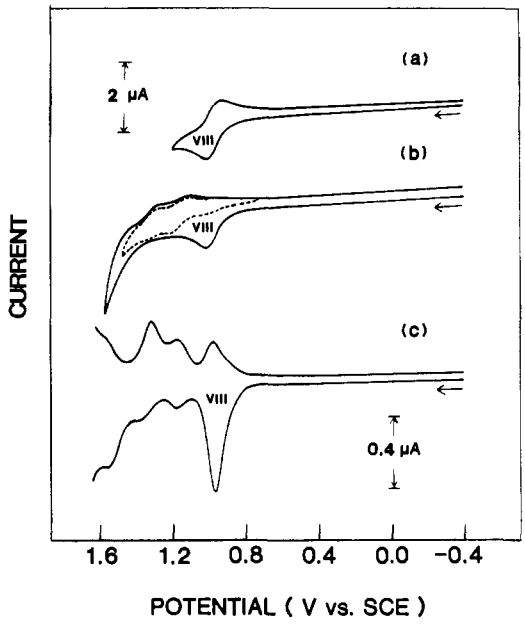

Figure 6. Cyclic voltammograms of 6.5×10^{-4} M (OEP)Nb(O)(O_2CCH_3) solution in CH_2Cl_2, 0.1 M TBAP. Scan rate = 0.1 V/s: (a) reversing scan at 1.20 V; (b) reversing scan at 1.60 V and also scanning positively a second time from 0.80 to 1.60 V (---). Part c shows differential pulse voltammogram scanned from −0.4 to +1.6 V and back. Scan rate = 10 mV/s.

two-electron process for the first step. This is consistent with an overlapping of currents for peaks VI and I. A small irreversible reoxidation wave occurs also in the cyclic voltammogram at $E_p \approx 0.18$ V, but this peak (peak III) is present only after the potential is scanned past the first reduction peak.

Figure 5b shows the cyclic voltammogram of (TPP)Nb(O)(acac) when the potential is varied over a range of +0.40 V to −1.70 V. Upon the second potential scan, two reversible processes (peaks I and II) are observed in the cyclic voltammogram. The first occurs at $E_{1/2} = -1.00$ V and has an $|E_{pa} - E_{pc}| = 60 \pm 5$ mV. The second process occurs at −1.39 V in CH_2Cl_2. Again, a reoxidation wave (peak III) is observed at 0.18 V.

The fact that reversible peaks I and II are observed for (TPP)Nb(O)(acac) on the second sweep as well as the occurrence of reoxidation peak III implies the formation of (TPP)Nb(O) after the first reduction. This assignment is supported by ESR spectra obtained from frozen solutions of (TPP)Nb(O)(acac) that were reduced at −1.28 V. The ESR signal is sensitive to the time of controlled-potential reduction, but the initial observed signal is characteristic of (TPP)Nb(O) and is similar to that shown in Figure 4. In agreement with the above results, chemical reduction of (TPP)Nb(O)(acac) with Zn/Hg also results in ESR spectra indicative of (TPP)Nb(O).

As the temperature is reduced from +22 to −74 °C, the first reduction of (TPP)Nb(O)(acac) (peak VI) becomes reversible (Figure 5c). Under these conditions the second reduction (peak VII) becomes irreversible and is observed at a more negative potential. At low temperature, peak VI has less current than peak VII. This is shown in Figure 5d and is in contrast to room-temperature experiments, where currents for the first reduction (peak VI) are greater than those of the second reduction (peak II).

Reversal of the potential scan at potentials negative of peak VII (Figure 5d) shows that the (TPP)Nb(O)(acac) starts to decompose after the second reduction and suggests that $acac^-$ remains bound after the first reduction at low temperature. The reversibility of peak VI at low temperatures indicates that the chemical reaction for cleavage of the Nb–acac bond is slowed down. Under these conditions, $[(TPP)Nb(O)(acac)]^-$ can then be further reduced to $[(TPP)Nb(O)(acac)]^{2-}$ (peak VII) before loss of $acac^-$ to form $[(TPP)Nb(O)]^-$.

Oxidation of (P)Nb(O)(O_2CCH_3). A cyclic voltammogram illustrating the oxidation of (OEP)Nb(O)(O_2CCH_3) in CH_2Cl_2 at 22 °C is shown in Figure 6a. A well-defined one-electron reversible oxidation (peak VIII) is observed at $E_{1/2} = 0.98$ V. However, if the potential is scanned to the solvent limit, as shown in Figure 6b, the return peak for the oxidation at 0.98 V is not observed. This is consistent with the report of irreversible oxidations for (P)Nb(O)(O_2CCH_3) and indicates the occurrence of a chemical reaction following the first oxidation.

The differential-pulse voltammogram of (OEP)Nb(O)(O_2CCH_3) in CH_2Cl_2 (Figure 6c) has a peak at $E_{1/2} = 0.98$ V, two smaller peaks at 1.18 and 1.37 V, and a larger peak at $E_p = 1.54$ V. The peaks following peak VIII are most likely due to oxidation of species generated by a homogeneous chemical reaction of $[(OEP)Nb(O)(O_2CCH_3)]^+$.

Reversible oxidation potentials for the (P)Nb(O)(O_2CCH_3) complexes in four solvents are presented in Table II. Similar electrochemical behavior is observed in CH_2Cl_2, PhCN, THF, and *n*-PrCN, although the rate of the chemical reaction following the first oxidation appears to be solvent-dependent. In all cases, the decomposition of $[(P)Nb(O)(O_2CCH_3)]^+$ is very rapid.

Spectroelectrochemical studies indicate that the first oxidation of (P)Nb(O)(O_2CCH_3) is at the porphyrin π ring system, but this electron transfer is followed by a rapid chemical reaction. Metal oxidation is not expected since Nb(VI) species are essentially unknown in solution chemistry.[16] Figure 7 demonstrates the changes that occur in the thin-layer electronic absorption spectrum upon oxidation of the acetate monomer at 1.00 V in benzonitrile. During electrooxidation the Soret band at 414 nm drops in intensity and shifts to 400 nm. In addition, the bands at 522, 538, 563, and 584 nm drop in intensity while new bands are observed at 535 and 568 nm. This spectrum corresponds to the product

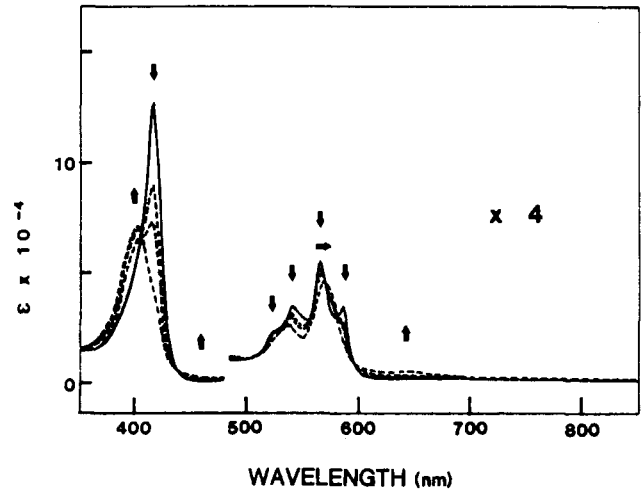

Figure 7. Thin-layer electronic absorption spectra of (OEP)Nb(O)(O_2CCH_3) in PhCN, 0.2 M TBAP during controlled-potential oxidation at 1.00 V for 0–5 min.

Table IV. Absorption Maxima (nm) and Molar Absorptivities (ϵ) of Oxidized (OEP)Nb(O)(O_2CCH_3) and (TPP)Nb(O)(O_2CCH_3) in PhCN Containing 0.2 M TBAP

compd	λ_{max}, nm ($10^{-4}\epsilon$)	
	neutral	ox 1
(OEP)Nb(O)(O_2CCH_3)	414 (12.7)	400 (7.0)
	522 (0.6)	535 (0.6)
	538 (0.8)	568 (1.1)
	563 (1.3)	
	584 (0.8)	
(TPP)Nb(O)(O_2CCH_3)	430 (29.9)	412 (12.2)
	533 (0.8)	
	555 (1.2)	

(16) Cotton, F. A.; Wilkinson, G. In *Advanced Inorganic Chemistry*, 4th ed.; Wiley: New York, 1980.

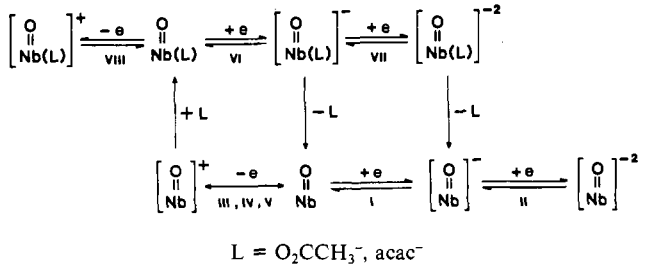

Figure 8. Overall scheme for the oxidation and reduction of (P)Nb(O) and (P)Nb(O)(L).

formed after the abstraction of one electron and the following chemical reaction.

Upon scans to more positive potentials, all spectral details of the (P)Nb(O)(O_2CCH_3) complex in solution are lost. Thus, the interpretation of the spectroelectrochemical data is that, following a ring-centered oxidation, decomposition of the acetate monomer takes place. This is consistent with the electrochemical data.

An ESR measurement on a frozen solution of (OEP)Nb(O)(O_2CCH_3) that was oxidized at +1.04 V in benzonitrile has a free-radical signal characterized by $g = 2.003$ and a signal width of 13 G. Approximately 1.0 electron was abstracted per monomer. This is in agreement with an oxidation occurring at the porphyrin ligand. However, further oxidation at potentials more positive than 1.4 V results in a different free-radical ESR signal, characterized by $g = 2.003$ and a width of 8 G. This radical is due to oxidation of the Nb porphyrin decomposition products.

Oxidation of (TPP)Nb(O)(acac). The oxidative behavior of (TPP)Nb(O)(acac) is similar to that of (TPP)Nb(O)(O_2CCH_3). It is characterized by a reversible oxidation wave at $E_{1/2} = 1.03$ V in CH_2Cl_2, 0.2 M TBAP. The wave has an $|E_{pa} - E_{pc}| = 60 \pm 5$ mV and an $i_p/v^{1/2}$ ratio that is constant, thus suggesting a diffusion-controlled, one-electron transfer. Rotating-disk experiments show that the current from the oxidation is about half that of the initial two-electron reduction, giving further support for the one-electron assignment in the oxidation.

If the potential is swept to more positive potentials, an irreversible wave is observed at $E_p = 1.48$ V. The characteristics of this wave are difficult to measure, since the oxidation of the complex occurs at potentials very close to the solvent discharge region. However, when the potential is scanned to this positive region, a return reduction peak is not observed for peak VIII.

The cyclic voltammetric data suggest the first oxidation product of (TPP)Nb(O)(acac) is stable on short time scales. However, after the second oxidation the compound appears to decompose. This is similar to the behavior of oxidized (P)Nb(O)(O_2CCH_3). The first oxidation is presumably at the porphyrin π ring system and not at the axial ligand, but this has not been demonstrated. At low temperatures, a reversible second oxidation of (TPP)Nb(O)(acac) appears to occur at $E_{1/2} = +1.38$ V, suggesting the decomposition of $[(P)Nb(O)(acac)]^+$ may be slower than $[(P)Nb(O)(O_2CCH_3)]^+$.

In conclusion, the oxidative and reductive behavior of (P)Nb(O)(L), where L = $acac^-$ or $O_2CCH_3^-$, are basically the same. Combining these data with the electrochemistry of (P)Nb(O) enables one to derive a complete electrochemical mechanism for the reduction of these complexes. This mechanism is shown in Figure 8.

The mechanism in Figure 8 involves a loss of the bound ligand on Nb(V) after generation of Nb(IV) and a set of noncoupled oxidation–reduction processes. Similar types of mechanisms are observed for metalloporphyrin complexes of Cr(III), Mn(III), Fe(III), and Mo(V).[15] In all cases, the reduction is shifted to potentials more negative than those of the uncomplexed species. The magnitude of this potential shift will depend upon how much the higher oxidation state is stabilized and is maximum for (TPP)Mo(O)(OCH_3).

The reductive behavior of the monomeric Nb(V) complexes is very similar to that of the dimeric Nb(V) complexes of the type $[(P)Nb]_2O_3$.[14] In both cases (P)Nb(O) is formed after reduction. This is not surprising, considering that the geometric arrangements of the three oxygen atoms about the niobium atom are very similar for all three complexes.[11,17,18] On a molecular orbital basis, the complexes should then have very similar electrochemical behaviors. However, the initial reduction of the dimers occurs at the porphyrin ring rather than at the metal center as observed for the monomeric Nb(V) porphyrins. Hence, formation of the same reduction product for both the dimers and monomers may only reflect the stability of (P)Nb(O).

Acknowledgment. The support of the National Science Foundation (Grant No. 8215507 and INT-8413696) and the CNRS (Grant No. 142) is gratefully acknowledged.

(17) Johnson, J. F.; Scheidt, W. R. *J. Am. Chem. Soc.* **1977**, *99*, 294.
(18) Johnson, J. F.; Scheidt, W. R. *Inorg. Chem.* **1978**, *17*, 1280.